Nanoscale

PAPER

View Article Online
View Journal | View Issue

Cite this: *Nanoscale*, 2014, **6**, 10734

High-efficiency transfer of percolating nanowire films for stretchable and transparent photodetectors†

Jiangxin Wang, Chaoyi Yan, Wenbin Kang and Pooi See Lee*

Received 6th May 2014
Accepted 7th July 2014

DOI: 10.1039/c4nr02462a

www.rsc.org/nanoscale

Stretchable devices with good transparency offer exciting new applications over the existing technologies, but remarkable difficulties remain in the fabrication of transparent and stretchable devices. In this paper, we report an effective method to fabricate transparent elastic photodetectors which combines the merits of the transparent polydimethylsiloxane (PDMS) polymer with its stretchability and the Zn_2SnO_4 nanowire (NW) with its photodetection functionality. Zonyl fluorosurfactant is found to be critical which improves the bonding between the functional NWs and the PDMS matrix, thus enabling the high efficient transfer of NW structures into PDMS. Highly conductive and thin percolating AgNW films were successfully embedded into PDMS mixed with ~11% Zonyl which are otherwise not achievable with pure PDMS. Transparent and stretchable photodetectors were fabricated with the developed method. The photocurrent was found to be reciprocal to the square of the channel length, $I_{ph} \sim 1/l^2$. The chemically bonded sensing materials in the PDMS matrix allow more NW exposure to air. This lead to a fast switching operation of the photodetectors with a response time below 0.8 s and a reset time around 3 s, which is significantly improved compared to reported stretchable NW photodetectors fully embedded in the polymer matrix.

Introduction

Stretchable electronics have recently received great attention in the research community.[1–6] Stretchable devices are "soft" electronic devices which can be deformed and wrapped onto nonplanar curved surfaces. They can mimic the mechanical compliance of human skin while a mass of additional functionalities can be integrated. Among them, stretchable photodetectors provide the function of converting light stimuli information into electrical signal. They enable the integrations with biological systems such as wearable monitoring devices, electronic eye cameras conformed to special curvilinear shapes, and infrared detectors for night vision[33–35] as well as many other applications. However, very limited reports can be found on stretchable photodetectors. Hemispherical imaging systems were demonstrated by utilizing thin and narrow wavy lines for connection between conventional rigid silicon sensing elements in their micrometer size.[7,8] Nanowires (NWs) have also been used to fabricate stretchable photodetectors with good stretchability up to 100%.[9] However, stretchable and meanwhile transparent photodetectors have not been achieved, despite the fact that good optical transparency will enable exciting novel applications, such as integrating with foldable screens, smart windows and other transparent electronics.

Polydimethylsiloxane (PDMS) is one of the most promising materials for stretchable electronics with good biocompatibility, high stretchability at room temperature, excellent optical transparency and ease of molding down to the nanometer scale.[10,11] Elastic conductors based on PDMS and conductive fillers (such as AgNWs) have been adopted as stretchable electric connections.[9,14] However, these elastic conductors were based on AgNW films up to several micrometer thick and thus were opaque. Thin and transparent AgNW films have not been demonstrated for stretchable conductors in these reports, probably due to the fact that the thin AgNW network could not be effectively transferred and embedded into the PDMS matrix. Large conductivity degradation might occur in the thin conducting network after the transfer process. Though AgNW embedded in poly(acrylate) has been demonstrated to achieve transparency and stretchability at the same time, the conductor required to be heated above its glass transition temperature (above room temperature) to become strechable.[12,13] Other approaches such as directly depositing thin NW networks on the top surface of PDMS might help to circumvent the problem,[15,16] but the exposed structures of the NW films make them mechanically vulnerable and tend to be easily displaced under repeated stretching.[17] The protruded NWs out of the substrate plane are also detrimental when a smooth surface is required for subsequent deposition of active layers in devices

School of Materials Science and Engineering, Nanyang Technological University, 50 Nanyang Avenue, Singapore 639798. E-mail: pslee@ntu.edu.sg

† Electronic supplementary information (ESI) available. See DOI: 10.1039/c4nr02462a

like light-emitting diodes (LEDs).[18,19] Here, we report a surfactant-assisted method to tackle the low-efficiency transfer of thin NW films into the PDMS elastomer matrix. High-efficiency transfer of thin percolating NW films enables the successful fabrication of stretchable and transparent NW photodetectors. The innovative approach can be widely applied for the fabrication of other stretchable or wearable devices.

Experimental

Transparent and stretchable conductor fabrication

AgNWs were purchased from Seashell Technology with diameters of 120–150 nm and lengths of 20–50 μm. The AgNW solution in isopropyl alcohol was diluted into a concentration of 0.5 mg ml^{-1} before use. The AgNW solution was deposited onto pre-cleaned glass substrates by a spray gun in the fume hood. Due to the fast evaporation rate of isopropyl alcohol, the spray-coated solution was immediately dried after being deposited onto the substrates without any heating. Pure PDMS was prepared by mixing the base and the curing agent (Sylgard 184, Dow Corning) with a ratio of 10 : 1. The liquid mixture was degassed and thermally cured at 60 °C overnight. Zonyl FS-300 fluorosurfactant was purchased from Sigma-Aldrich and used as received. The PDMS base, curing agent and Zonyl were mixed in different weight ratios of 10 : 2 : 1, 10 : 2 : 1.5, and 10 : 2 : 2. The mixture composition of 10 : 2 : 1.5 showed good bonding between the PDMS matrix and AgNWs without affecting the stretchability of PDMS. SEM images of the surfaces of AgNW/PDMS mixed with different Zonyl concentrations are shown in ESI Fig. S1.†

Fig. 1a illustrates the fabrication procedure of a stretchable transparent conductor. Initially, the AgNW solution was spray-coated onto a pre-cleaned glass substrate to form a homogenous interconnecting NW network, as shown in the SEM image of Fig. 1b. The AgNW network was annealed at 200 °C for 20 min to remove the polyvinylpyrrolidone (PVP) capping agent on the NW surface and create fusion between the AgNWs.[20] Sheet resistivity of the AgNW films was significantly reduced after the annealing process. Liquid PDMS mixed with different amounts of fluorosurfactant Zonyl-FS300 (Zonyl) was poured onto the AgNW coated substrate, degassed for 30 min in a vacuum desiccator to allow the liquid to penetrate and wrap around the NW network. After that, the samples were transferred into an oven to cure the PDMS overnight at 110 °C. The resultant AgNW/PDMS conductors were peeled off from the glass substrate for further characterization. Fig. 1c shows a transparent stretchable conductor with homogenously coated AgNW films.

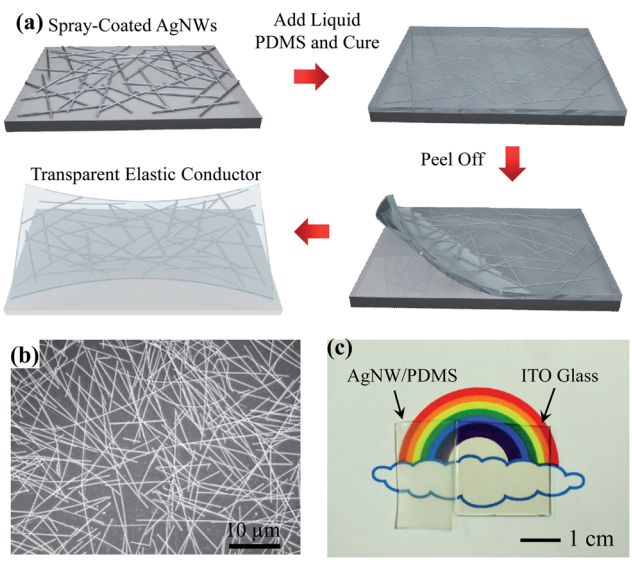

Fig. 1 (a) Fabrication procedure of the transparent stretchable conductor. (b) SEM image of a highly conductive AgNW film coated on glass substrate. (c) Optical photograph of the AgNW/PDMS stretchable conductor with a sheet resistivity of 4.5 Ω sq^{-1}, comparing with ITO glass with a sheet resistivity of 10 Ω sq^{-1}.

Photodetector fabrication

Zn_2SnO_4 NWs were synthesized by a chemical vapor deposition method.[32] The synthesized Zn_2SnO_4 NWs were removed from the silicon substrate and dispersed into isopropanol alcohol solution with a concentration of ~0.1 mg ml^{-1}. The Zn_2SnO_4 NW solution was sonicated for 15 minutes before use. Morphologies of the Zn_2SnO_4 NWs are shown in ESI Fig. S3.† Zn_2SnO_4 NWs and AgNWs were coated onto glass substrates through the shadow masks subsequently to form the photodetector electrode and detection channel arrays. The devices were then transferred into the PDMS matrix by the method developed above.

Characterization

SEM images of the samples were taken using a field-emission SEM (FE-SEM, JSM 7600F). The transmittance spectra were measured using a Shimadzu spectrometer (UV-3600) equipped with an optical integration sphere. The strain tests of the stretchable conductors and photodetectors were both carried out on a home-made stretching stage at room temperature. The electrical properties of the photodetector were characterized using a Keithley 4200-SCS parameter analyzer. The UV light with a central wavelength of 254 nm was generated using a portable UV lamp.

Results and discussion

Glass substrates coated with similar densities of AgNWs were used to study the effect of Zonyl on the NW transfer efficiency. First we studied the transfer into a pure PDMS matrix without the Zonyl surfactant. Surfaces of the AgNW/PDMS conductors were characterized with SEM after being peeled off from the glass substrates. The peeled surface of AgNWs embedded in pure PDMS, as shown in Fig. 2a, has significantly reduced the wire density compared to the as-coated network on the glass substrate (Fig. 1b). The AgNWs distribute sparsely in the PDMS matrix with limited interconnection nodes. The resultant conductor had poor conductivity, which was beyond the measurement range of our equipment. Though the thickness of the AgNW films increased with the sample transparency

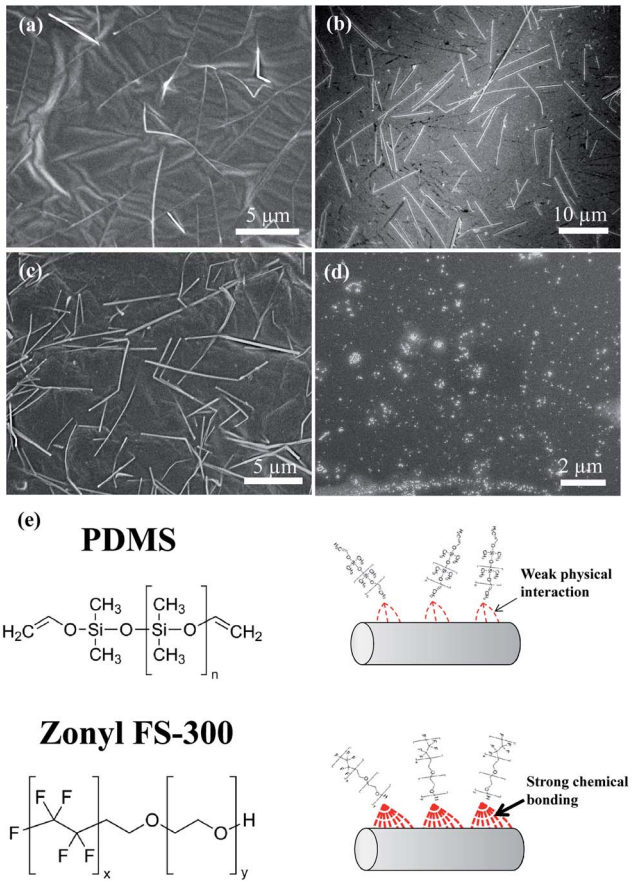

Fig. 2 (a) SEM image of the surface of AgNWs in pure PDMS after being peeled off from the glass substrate. (b) Top surface image of the glass substrate after peeling off the AgNW/PDMS without Zonyl. (c) SEM image of the surface of the AgNW/PDMS elastic conductor with ~11 wt% Zonyl after being peeled off from glass. (d) Top surface image of the glass substrate after peeling off the AgNW/PDMS elastic conductor with ~11 wt% Zonyl. (e) Chemical structures of PDMS and Zonyl. The schematic on the right illustrates their distinct interactions with AgNWs.

dramatically reduced below ~40%, no substantial improvement in the conductivity could be observed. To investigate the cause of weak conductivity, we inspected the surface of the exposed glass substrate after the transfer process. As represented in Fig. 2b, the SEM image shows that substantial amounts of AgNWs remain on the glass substrate, revealing clearly a non-ideal NW transfer efficiency. Highly conductive AgNW/PDMS conductors have been reported by embedding AgNW films with thickness of several micrometers.[9,14] In these cases, the conductive pathways are established through the massive NW–NW junctions. Although peeling off of the polymer composite from the substrate would sacrifice NWs on the top surface, the NW network can still retain its good conductivity with the large amount of interconnecting AgNWs in the bulk. To achieve an optically transparent conductor, however, a much thinner film of AgNWs is required (monolayer or few layers as shown in Fig. 1b). Consequently, damage to the conductive film during the embedding process will result in severe conductivity degradation. PDMS is well-known for its very low surface energy of ~20 mN m^{-1}.[21] The transfer can only be effective when most part of the NW is embedded within the PDMS polymer, as schematically shown in Fig. S2, ESI.† SEM observations also verified that most of the NWs successfully transferred into the pure PDMS matrix (without Zonyl surfactant) were fully embedded inside the PDMS (see comparison in Fig. 2c with plenty of exposed NWs). Those AgNWs that are close to the interface will remain on the supporting substrate due to the weak physical interaction between the AgNWs and PDMS. To achieve a high-efficiency transfer of the transparent AgNW film, stronger bonding between the NWs and PDMS is required. The Zonyl fluorosurfactant has an amphiphilic nature with both fluorinated and ethylene glycol segments (Fig. 2e). It has been used to effectively improve the interaction between PEDOT:PSS and PDMS.[22,23] The ethylene glycol group enables chemical coupling with the AgNW surface through O–Ag bonding[24,25] and is expected to improve the bonding strength between the PDMS matrix and AgNWs. Indeed, with the addition of ~11 wt% Zonyl, significantly improved transfer efficiency for AgNWs at the interface was observed as shown in Fig. 2c. The surfactant-assisted highly efficient transfer was further verified by the SEM characterization in Fig. 2d, showing that all the NWs have been transferred from the substrate. A smaller ratio of Zonyl had similarly shown increased transfer efficiency compared to pure PDMS while ~11 wt% Zonyl was demonstrated to offer the best transfer efficiency in our study. Continuous increase of the Zonyl ratio may not increase the transfer efficiency. On the contrary, excess Zonyl will affect the mechanical properties of the PDMS matrix and lead to an inferior surface roughness of the polymer. The effects of different Zonyl ratios were further discussed in the ESI (Fig. S1†). The chemical structures of PDMS and Zonyl as well as their distinct interactions with the AgNWs are presented in Fig. 2e.

Fig. 3a shows the transmission spectra of the AgNW elastic conductor. The highly conductive AgNW/PDMS composite, with a sheet resistivity of 4.5 Ω sq^{-1}, has a transmittance of 80% at 550 nm which is comparable to commercial ITO/glass (10 Ω sq^{-1}, ~85% transmittance). Transparency of the elastic conductor can be further improved by using AgNWs with higher aspect ratio.[26] The elastic conductor was stretched up to 100% and resistance changes were measured. Fig. 3b shows the resistance variation $\Delta R/R_0$ ($\Delta R = R - R_0$, R is the measured resistance under different strains, R_0 is the initial resistance before stretching) upon stretching. The conductor could maintain good conductivity even at 100% tensile strain. The resistance first increased slowly before 50% strain, which was mainly due to the increasing length of the conducting path. Beyond the stretching strain of 50%, the resistance change became more significant with $\Delta R/R_0$ reaching 32.8 at 100% strain. The resistance change followed a similar trend when the conductor was released. More stretching tests were performed on a new sample in the strain range of 0–50%, as presented in Fig. 3c. Though there was a slight increase in the resistivity as the stretching cycles increased, the conductor could still maintain the conductive path under reversible stretching. Current was passed through the elastic conductor to power a LED, as shown in Fig. 3d. The LED remained lit when the

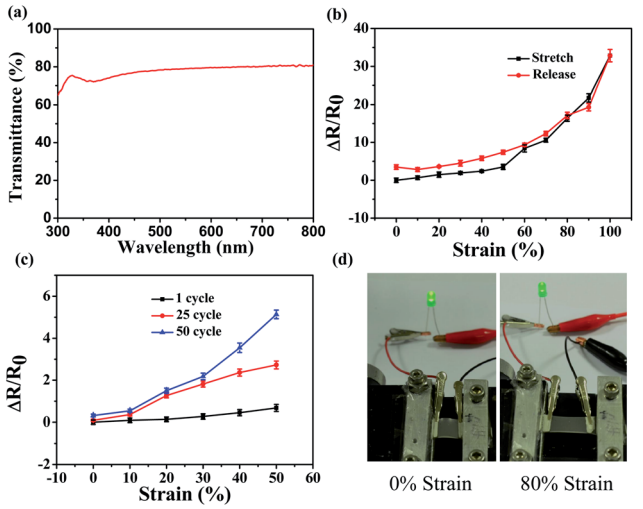

Fig. 3 (a) Transmittance spectra of the AgNW/PDMS stretchable conductor. (b) Resistance change of the AgNW/PDMS conductor as a function of tensile strain. (c) Resistance change in the stretchable conductor as a function of tensile strain at the first, twenty-five and fifty stretching cycles. (d) Photographs of a powered light-emitting diode integrated with the elastic conductor under tensile strains of 0% and 80%.

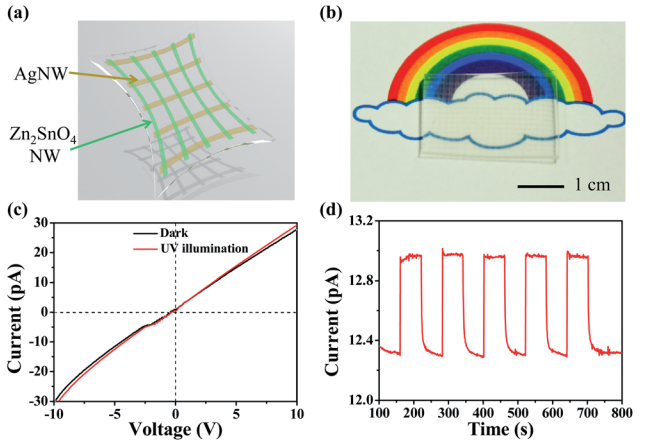

Fig. 4 (a) A schematic of the stretchable transparent UV photodetector. (b) A photograph of the stretchable elastic photodetector. (c) *I*–*V* curves of the unstrained photodetector under dark and UV illumination conditions. (d) Dynamic current–time measurement of the device with periodical on/off UV light.

conductor was stretched to 80% strain. Brightness of the LED reduced due to increased resistivity of the conductor under the stretched state. Performance of the stretchable conductor is much better comparable to previously reported AgNW films on PDMS substrates.[16,17] The performance is also comparable to the distinguished studies in the literatures which use other stretchable polymer matrices for the embedding process.[2,12]

The surfactant-assisted transfer method is shown to be effective to fabricate a PDMS-based transparent elastic conductor. The functionality of the NW films can be maintained, while the stretchability can be imparted simultaneously by the PDMS matrix. Stretchable and transparent photodetector arrays based on conducting AgNW films and semiconducting Zn_2SnO_4 NW films were successfully demonstrated with the developed method. AgNWs were first spray-coated onto the glass substrate through a shadow mask. Subsequently, the shadow mask was rotated by an angle of 90 °C and used to coat the light sensing materials. Other device configurations can also be realized by using different shadow masks. Zn_2SnO_4 NWs were used for the sensing material as they have high sensitivity and selectivity to the Ultraviolet (UV) light.[27] Fig. 4a presents the schematic of the device. The Zn_2SnO_4 NW active channel, with a length of 0.5 mm, was formed between the two parallel AgNW lines. Fig. 4b shows a stretchable photodetector device with high transparency. The transmittance spectrum of the device can be found in ESI Fig. S4.† *I*–*V* curve of the device in Fig. 4c indicates good ohmic contact between the AgNWs and the Zn_2SnO_4 NWs. The device current under a dark environment and UV light illustration are also shown in Fig. 4c. The large dark current of the photodetector, 12.3 pA at the bias of 5 V, can be attributed to the high carrier density, good mobility in the Zn_2SnO_4 NWs or the large device area. Dynamic performance of the device, biased with 5 V, is shown in Fig. 4d. The UV light was turned on and off both for 60 s periodically. The device shows fast response to the UV light and good cyclic stability.

Performance of the photodetector was examined when the device was uniaxially stretched along the direction of the channel length. Fig. 5a shows images of the photodetector under 0%, 20% and 50% strains respectively. Photoresponse of the device is shown in Fig. 5b. The device demonstrates stable response up to the tensile strain of 50%, while the photocurrent decreases as the strain value increases. Photoresponse behavior of the device can be understood through the electron–hole separation upon excitation by the incident photons. These electrons are either collected by the electrodes (contribute to the photocurrent) or recombine with holes in the channel (do not

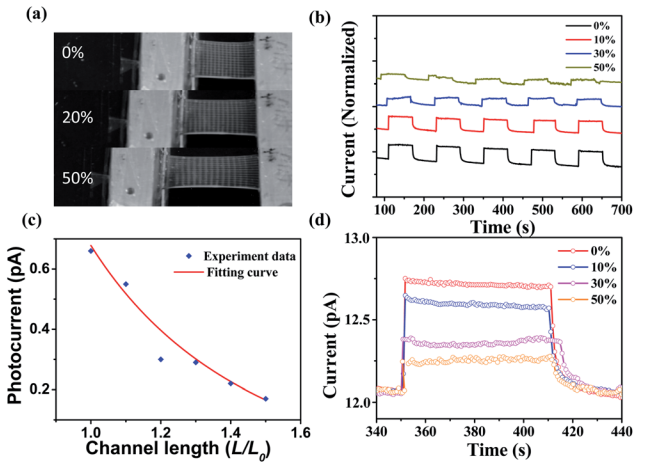

Fig. 5 (a) Digital photographs of the stretchable photodetector under a stretching test. (b) Response of the device at tensile strains of 0%, 10%, 30%, and 50%. (c) Fitting of the photocurrent at different tensile strains. (d) Magnification of the photocurrent responds with an enlarged on/off cycle at tensile strains of 0%, 10%, 30%, and 50%.

contribute to the photocurrent). Consequently, the lifetime of the photo-generated carriers τ and the transit time of the carriers τ_t are two critical parameters for the photodetector behavior. The photoconductive gain G can be evaluated by the following equation:[28,29]

$$G = \frac{\tau}{\tau_t} = \frac{\mu V \tau}{l^2} \quad (1)$$

where $\tau_t = l^2/\mu V$ (l is the channel length of the device, μ is the carrier mobility and V is the applied voltage). The photocurrent gain is proportional to the photocurrent I_{ph} ($I_{ph} = I_{illumination} - I_{dark}$):[30,31]

$$G = \frac{I_{ph}/q}{P_{opt}/hv} \quad (2)$$

where P_{opt} is the absorbed optical power, q is the elementary charge, h is the Planck constant, and v is the frequency of the absorbed photon. By combining eqn (1) and (2), one can obtain:

$$I_{ph} = \frac{P_{opt} q \mu V \tau}{hvl^2} \quad (3)$$

From eqn (3), it can be concluded that the photocurrent is reciprocal to the square of the channel length with constant incident light power and applied voltage. Fig. 5c plots the photocurrent changes against the channel length. The line fitting, red line in Fig. 5c, is performed on the experiment data, showing good agreement with the relationship between the photocurrent and the channel length as deduced above. The magnified photocurrent in a single on/off cycle shows fast response time of the elastic photodetector. Within 0.8 s, which is limited by the measuring time of our equipment, the photocurrent of the device jumps to the maximum value after the detection light is on. The reset time is defined as the time required for the photocurrent to decrease to $1/e$ (37%) of the maximum value, which is ~3 s for the device. No clear dependence of the time response on the tensile strains was observed. The photoresponse behavior is faster compared to reported stretchable NW photodetector,[9] which has a response time of ~30 s and reset time of ~6 s at 0% strain. The response/reset time will further increase with increased strains. The switching speed of this device is hindered by the oxygen deficient environment with the device structures fully embedded in the PDMS matrix. When the device is stretched, the contact area between the NWs and air will be further decreased (a more oxygen deficient environment), leading to an increased response/reset time. The transparent elastic photodetector reported here has a chemically bonded device structure with more NW surface exposed to air. The contact area changes between the functional NWs and air are negligible upon stretching. Consequently, a fast and stable photoresponse time was observed. Its switching speed is close to that of the reported Zn_2SnO_4 NW photodetector fabricated on the SiO_2/Si substrate (response time/reset time: 0.46 s/0.42 s).[27] Stretching the device along the channel width up to 50% shows almost no change in the photocurrent and photoresponse time, corroborating the mechanism illustrated. The cycling stability test of the device stretched along the channel length direction was also carried out. Detailed results and discussion can be found in the ESI (Fig. S5†).

Conclusions

In summary, we have demonstrated an effective method to fabricate transparent and stretchable photodetectors. The elastic photodetector is based on embedded device structures in the PDMS matrix to render stretchable capability to the rigid inorganic materials while the functionality of the device is preserved. To reduce damage to the device structures when peeled off from the supporting substrates, a Zonyl fluorosurfactant was added to the PDMS liquid. The introduced ethylene glycol group from Zonyl greatly increases the bonding strength between the rubber matrix and the NW surface. A stretchable and transparent conductor was fabricated with a sheet resistivity of 4.5 Ω sq^{-1} and a transmittance of 80% at 550 nm. Following a similar procedure, a transparent elastic UV photodetector was also demonstrated. The photodetector has stable performance with the tensile strain up to 50%. The photocurrent is reciprocal to the square of the channel length, $I_{ph} \sim 1/l^2$. The photodetector has a prompt response time below 0.8 s and a fast reset time of ~3 s. Combining its good transparency and stretchability, the elastic photodetector may find broad applications when integrated with clothes, skins and organs for wearable and implantable electronics which are unreachable with conventional rigid technologies.

Acknowledgements

The authors thank V. Bhavanasi, M. F. Lin and X. Wang for their technical support and insightful discussions. The authors would like to acknowledge the funding support from NTU-A*Star Silicon Technologies Centre of Excellence under the program grant no. 112 3510 0003.

References

1 R. H. Kim, D. H. Kim, J. L. Xiao, B. H. Kim, S. I. Park, B. Panilaitis, R. Ghaffari, J. M. Yao, M. Li, Z. J. Liu, V. Malyarchuk, D. G. Kim, A. P. Le, R. G. Nuzzo, D. L. Kaplan, F. G. Omenetto, Y. G. Huang, Z. Kang and J. A. Rogers, *Nat. Mater.*, 2010, **9**, 929–937.
2 J. J. Liang, L. Li, X. F. Niu, Z. B. Yu and Q. B. Pei, *Nat. Photonics*, 2013, **7**, 817–824.
3 W. H. Yeo, Y. S. Kim, J. Lee, A. Ameen, L. K. Shi, M. Li, S. D. Wang, R. Ma, S. H. Jin, Z. Kang, Y. G. Huang and J. A. Rogers, *Adv. Mater.*, 2013, **25**, 2773–2778.
4 T. G. McKay, B. M. O'Brien, E. P. Calius and I. A. Anderson, *Appl. Phys. Lett.*, 2011, **98**, 142903.
5 D. J. Lipomi, M. Vosgueritchian, B. C. K. Tee, S. L. Hellstrom, J. A. Lee, C. H. Fox and Z. N. Bao, *Nat. Nanotechnol.*, 2011, **6**, 788–792.
6 S. Xu, Y. H. Zhang, J. Cho, J. Lee, X. Huang, L. Jia, J. A. Fan, Y. W. Su, J. Su, H. G. Zhang, H. Y. Cheng, B. W. Lu, C. J. Yu, C. Chuang, T. I. Kim, T. Song, K. Shigeta, S. Kang,

C. Dagdeviren, I. Petrov, P. V. Braun, Y. G. Huang, U. Paik and J. A. Rogers, *Nat. Commun.*, 2013, **4**, 1543.
7 H. C. Ko, M. P. Stoykovich, J. Song, V. Malyarchuk, W. M. Choi, C. J. Yu, J. B. Geddes, 3rd, J. Xiao, S. Wang, Y. Huang and J. A. Rogers, *Nature*, 2008, **454**, 748–753.
8 Y. M. Song, Y. Xie, V. Malyarchuk, J. Xiao, I. Jung, K. J. Choi, Z. Liu, H. Park, C. Lu, R. H. Kim, R. Li, K. B. Crozier, Y. Huang and J. A. Rogers, *Nature*, 2013, **497**, 95–99.
9 C. Yan, J. Wang, X. Wang, W. Kang, M. Cui, C. Y. Foo and P. S. Lee, *Adv. Mater.*, 2013, **26**, 943–950.
10 D. H. Kim, R. Ghaffari, N. S. Lu and J. A. Rogers, *Annu. Rev. Biomed. Eng.*, 2012, **14**, 113–128.
11 D.-H. Kim, N. Lu, Y. Huang and J. A. Rogers, *MRS Bull.*, 2012, **37**, 226–235.
12 W. Hu, X. Niu, L. Li, S. Yun, Z. Yu and Q. Pei, *Nanotechnology*, 2012, **23**, 344002.
13 S. Yun, X. Niu, Z. Yu, W. Hu, P. Brochu and Q. Pei, *Adv. Mater.*, 2012, **24**, 1321–1327.
14 F. Xu and Y. Zhu, *Adv. Mater.*, 2012, **24**, 5117–5122.
15 M. S. Lee, K. Lee, S. Y. Kim, H. Lee, J. Park, K. H. Choi, H. K. Kim, D. G. Kim, D. Y. Lee, S. Nam and J. U. Park, *Nano Lett.*, 2013, **13**, 2814–2821.
16 T. Akter and W. S. Kim, *ACS Appl. Mater. Interfaces*, 2012, **4**, 1855–1859.
17 M. S. Miller, J. C. O'Kane, A. Niec, R. S. Carmichael and T. B. Carmichael, *ACS Appl. Mater. Interfaces*, 2013, **5**, 10165–10172.
18 L. Hu, H. S. Kim, J.-Y. Lee, P. Peumans and Y. Cui, *ACS Nano*, 2010, **4**, 2955–2963.
19 J.-Y. Lee, S. T. Connor, Y. Cui and P. Peumans, *Nano Lett.*, 2008, **8**, 689–692.
20 A. R. Madaria, A. Kumar, F. N. Ishikawa and C. Zhou, *Nano Res.*, 2010, **3**, 564–573.
21 D. Fuard, T. Tzvetkova-Chevolleau, S. Decossas, P. Tracqui and P. Schiavone, *Microelectron. Eng.*, 2008, **85**, 1289–1293.
22 M. Vosgueritchian, D. J. Lipomi and Z. Bao, *Adv. Funct. Mater.*, 2012, **22**, 421–428.
23 D. J. Lipomi, J. A. Lee, M. Vosgueritchian, B. C. K. Tee, J. A. Bolander and Z. Bao, *Chem. Mater.*, 2011, **24**, 373–382.
24 Y. Sun, Y. Yin, B. T. Mayers, T. Herricks and Y. Xia, *Chem. Mater.*, 2002, **14**, 4736.
25 H. H. Huang, X. P. Ni, G. L. Loy, C. H. Chew, K. L. Tan, F. C. Loh, J. F. Xu and G. Q. Deng, *Langmuir*, 1996, **12**, 909.
26 L. B. Hu, H. S. Kim, J. Y. Lee, P. Peumans and Y. Cui, *ACS Nano*, 2010, **4**, 2955–2963.
27 Y. J. Zhang, J. J. Wang, H. F. Zhu, H. Li, L. Jiang, C. Y. Shu, W. P. Hu and C. R. Wang, *J. Mater. Chem.*, 2010, **20**, 9858–9860.
28 O. Lopez-Sanchez, D. Lembke, M. Kayci, A. Radenovic and A. Kis, *Nat. Nanotechnol.*, 2013, **8**, 497–501.
29 C. Soci, A. Zhang, X. Y. Bao, H. Kim, Y. Lo and D. L. Wang, *J. Nanosci. Nanotechnol.*, 2010, **10**, 1430–1449.
30 C. Soci, A. Zhang, B. Xiang, S. A. Dayeh, D. P. R. Aplin, J. Park, X. Y. Bao, Y. H. Lo and D. Wang, *Nano Lett.*, 2007, **7**, 1003–1009.
31 G. Cheng, X. H. Wu, B. Liu, B. Li, X. T. Zhang and Z. L. Du, *Appl. Phys. Lett.*, 2011, **99**, 203105.
32 T. Lim, H. Kim, M. Meyyappan and S. Ju, *ACS Nano*, 2012, **6**, 4912–4920.
33 J. Wu, D. Shao, V. G. Dorogan, A. Z. Li, S. Li, E. A. DeCuir, Jr., M. O. Manasreh, Z. M. Wang, Y. I. Mazur and G. J. Salamo, *Nano Lett.*, 2010, **10**, 1512–1516.
34 B. S. Passmore, J. Wu, M. O. Manasreh, V. P. Kunets, P. M. Lytvyn and G. J. Salamo, *IEEE Electron Device Lett.*, 2008, **29**, 224–227.
35 E. Cicek, R. McClintock, Z. Vashaei, Y. Zhang, S. Gautier, C. Y. Cho and M. Razeghi, *Appl. Phys. Lett.*, 2013, **102**, 051102.